



Modulation of the Photophysical Properties of β -substituted BODIPY Dyes

Ankush B. More¹ · Goutam Chakraborty² · Soumyaditya Mula³ · Alok K. Ray² · Nagaiyan Sekar¹

Received: 29 July 2017 / Accepted: 7 December 2017
© Springer Science+Business Media, LLC, part of Springer Nature 2017

Abstract

Photophysical properties of BODIPY dyes containing acetyl acetone and benzoyl acetone BF₂ unit as an electron accepting substituent at beta position linked via double bond have been investigated using a wide range of solvents of different polarities. The substitution effect at beta position of the BODIPY dyes on their absorption, emission and quantum yield of fluorescence have been the aim of present study. For the synthesized BODIPY dyes fluorescence quantum yields and lifetimes show very sharp decrease with an increase in the solvent polarity, suggesting the involvement of highly polar ICT state de-excitation mechanism along with the local excitation process. The polarity dependent changes in average fluorescence life time and quantum yield values rationalize the formation of ICT states.

Keywords BODIPY · ICT · Radiative and nonradiative process and DFT

Introduction

Organic Luminescent dyes constrained cyanines such as BODIPY, aza-BODIPY, and boranil derivatives have become key tools for biological, medicinal and analytical applications due to their excellent photophysical properties [1, 2]. Indeed, the widespread applications of the difluoroboron complexes in several fields, for example ion sensing [3], nonlinear optics [4], photodynamic therapy [5] as well as biomedical indicators [6], fluorescence imaging [7] and dye lasers [8] have attracted attention of many researchers over the years. Compared to others dyes which are used in the visible spectral region (e.g., rhodamine, coumarin, oxazine), the borondipyromethene

(BODIPY) has several advantages over the other fluorophore in view of their high absorption coefficients in the similar spectral region, robust chemical properties, high fluorescence quantum yields, low triplet to triplet conversion efficiency and good thermal and photostability [3, 8]. These properties of BODIPYs make them as very efficient choice for the active medium in the dye lasers. The main drawback concerning BODIPY is small Stokes shift which sometimes limits the use of BODIPY as dyes laser due to self-absorption phenomena. There are substantial efforts to improve the Stokes shift of BODIPY dyes by introducing different substituents in the BODIPY core so that BODIPYs can be effectively used as laser dyes where there is a compulsory criteria to have large Stokes shift. In the last few decades BODIPY dyes have gained considerable attention of the scientists all over the world due to their ease of functionalization at the desired position of the BODIPY core which includes base catalyzed aldehyde condensation [9–11], transition metal catalyzed cross-coupling reactions [12, 13] and nucleophilic substitutions [14]. Amongst all the reactions which bring the changes in the BODIPY functionalization. An interesting way in this context is to have an extended conjugation and the donor acceptor balance between the BODIPY core with the substituent which results in the shift of the absorption and emission spectra towards red region. Several research groups have also developed a synthetic approach which

Electronic supplementary material The online version of this article (<https://doi.org/10.1007/s10895-017-2200-5>) contains supplementary material, which is available to authorized users.

✉ Nagaiyan Sekar
n.sekar@ictmumbai.edu.in; neti.sekar@gmail.com

¹ Department of Dyestuff Technology, Institute of Chemical Technology, Mumbai 400019, India

² Laser and Plasma Technology Division, Bhabha Atomic Research Centre, Mumbai 400085, India

³ Bio-Organic Division, Bhabha Atomic Research Centre, Mumbai 400085, India

is based on a Knoevenagel type condensation between selected aldehyde and a BODIPY comprising two methyl groups in the 3 and 5 positions. However, these condensations usually proceed in low yields [15]. In view of this, the Knoevenagel condensation of BODIPY aldehyde with active methyl group is achieved in excellent yields [9]. There are ample reports on 8- and 3- or 3,5- substituted BODIPYs but not much work has been done on 2-substituted BODIPYs, especially with electron acceptor moieties. The borondifluoride complexes of acetyl acetone(acac), benzoyl acetone(bzac) and their respective curcuminoids congeners are the strong electron donor–acceptor (D-A) system [16]. In the present study, we report the synthesis and luminescence properties of β -substituted BODIPY dyes with conjugated electron acceptor moieties linked to BODIPY dyes at beta position via condensation reaction between formyl BODIPY and boron complexes of acac and bzac. The influence of the electron accepting character of the boron complexes of acetyl acetone and benzoyl acetone with their respective curcuminoids congeners are studied using UV–visible, steady state and time-resolved fluorescence spectroscopy techniques, and supported by quantum chemical calculations. Moreover, the formation of intramolecular charge transfer (ICT) states is supported by experimental results that show a sharp decrease in fluorescence quantum yields and lifetimes with increasing solvent polarity.

Materials and Methods

The chemicals and spectroscopic grade solvents were procured and used as such without further purifications unless otherwise mentioned. All the common chemicals were of analytical grade. The reaction progress were monitored by TLC (thin-layer chromatography). The steady state spectroscopic measurements were carried out using UV–vis spectrophotometer and fluorimeter HORIBA fluormax Time resolved studies were performed using HORIBA TCSPC instrument. HRMS analysis was obtained using a 6550 iFunnel QTOF LC/MS, 1290 infinity Binary pump. ^1H NMR, ^{13}C NMR, spectra were recorded on a 500 MHz Agilent instrument using TMS as an internal standard. All the quantum chemical computations were performed using the Gaussian 09 program package [17]. The ground state (S_0) geometries of the dyes were optimized using the density functional theory (DFT) method. The first excited (S_1) states were optimized using time dependent density functional theory (TD-DFT) [18]. The functional used was B3LYP (the B3LYP combines Becke's three parameter exchange functional (B3) with the nonlocal correlation functional by Lee, Yang and Parr (LYP)) [19].

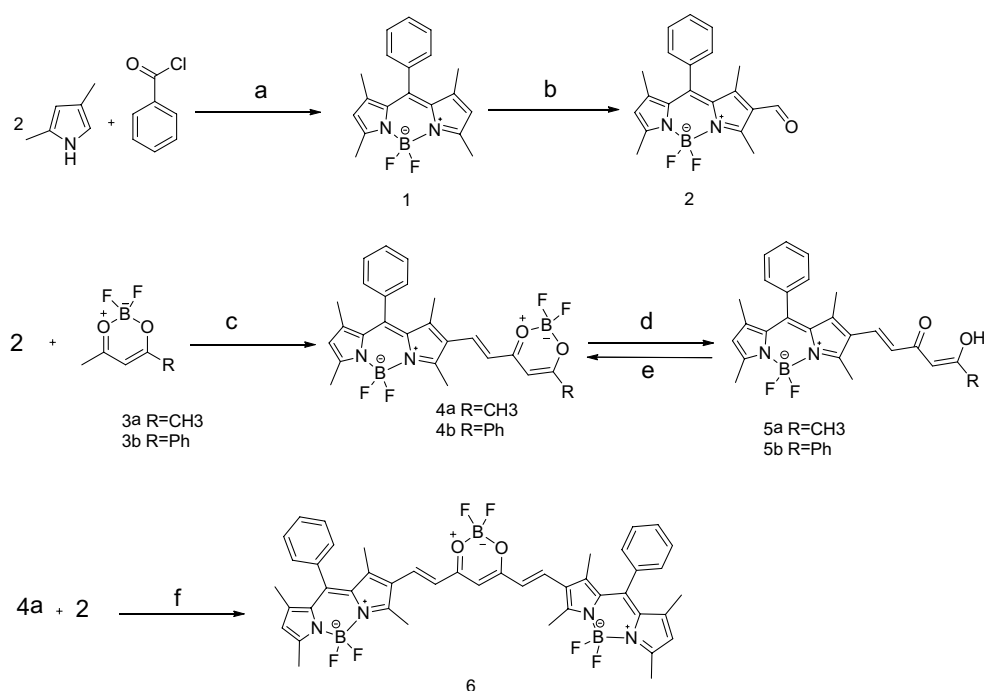
Results and Discussion

Synthesis

The synthesis route proceeds with the known BODIPY dye **1** [20], which was converted to dye **2** via selective β -formylation using Vilsmeier-Haack reaction by the synthetic procedure reported in *ref* [21]. The β -formyl BODIPY **2** on further condensation with acetylacetone difluoroboron complex **3a** and benzoylacetone difluoro-complex **3b** furnished dyes **4a** and **4b**, respectively [22]. It is worth noting that the acac-BF₂ as well as bzac -BF₂ unit in **4a** and **4b** were regio-selectively removed by refluxing in MeOH/DMSO to obtain dye **5a** [23] and **5b** (Scheme 1) [22]. The BF₂ unit of BODIPY moiety remained intact under the reaction conditions, as revealed from its NMR spectra and HRMS data. Further the dyes **4a** and **4b** were synthesized in very good yield reversibly from dyes **5a** and **5b** upon reaction with BF₃.OEt₂ in dry DCM. The second methyl group of acetyl acetone unit of the dye **4a** was further condensed with dye **2** to get BODIPY dimer **6**. Unfortunately, decomplexation of the BODIPY dimer **6** offer dye with least solubility in almost all solvents, this limits the characterization of the dye, hence not discussed in the present study.

Photophysical Properties

The photophysical properties such as ground state absorption, steady state as well as time resolved fluorescence measurements of the five dyes **4a**, **4b**, **5a**, **5b** and **6** were evaluated at 25 °C using solvents of different polarities. The measured photophysical parameters (longest wavelength absorption maximum (λ_{abs}), emission maximum (λ_{em}), quantum yield of fluorescence (Φ_{F}), and the calculated Stokes shift (ν)) of the dyes are presented in Table 1. The normalized absorption and emission spectra of the dyes **4a**, **4b**, **5a**, **5b** and **6** in dichloromethane are shown in Fig. 1. The acac BF₂ BODIPY dye **4a** shows absorption maxima at 551 nm and emission maxima at 572 nm where as bzac BF₂ BODIPY **4b** shows absorption maxima at 567 nm and emission maxima at 595 nm. The extended conjugation of phenyl ring in dye **4b** cause a bathochromic shift of 16 nm in absorption and 23 nm in emission peaks in comparison with dye **4a**. Further on removal of BF₂ from OBO complex, the BODIPY dyes **5a** and **5b** shows a blue shift in absorption maxima compared with their parent dyes **4a** and **4b**. This concludes the functionalization of these groups also affects to the rigidity of the chromophore and hence, the structural changes also have major influence on the photophysical properties. The



Scheme 1 Synthesis. Reagents and conditions: (a) dry DCM, TEA/ $\text{BF}_3 \cdot \text{Et}_2\text{O}$, RT, 12 h; (b) DMF/ POCl_3 /DCE, 60 °C, 3 h; (c) n-Butyl amine/tri butyl borate, toluene, 70 °C, 16 h. (d) MeOH/DMSO,

95 °C, 3 h; e) TEA/ $\text{BF}_3 \cdot \text{Et}_2\text{O}$, RT, 12 h; f) n-Butyl amine/tri butyl borate, toluene, 70 °C, 16 h

extended conjugation of phenyl ring of the bzac unit in dye **4b** causes the red shifted emission and is more prominent in polar solvents (≈ 600 nm). The normalized absorption and emission spectra of dyes **4a** and **4b** are presented in Figs. 2, 3 and for **5a**, **5b** and **6** in S1, S2 and S3. Considerably the extended conjugation in case of BODIPY dimer **6** offers red shift both in λ_{abs} and λ_{em} shows λ_{abs} at 624 nm and λ_{em} at 658 nm.

The fluorescence quantum yield (Φ_{F}) values for BODIPY dyes in different solvents were estimated using a comparative method and the values thus estimated are listed in Table 1. Figure 4a, b show the solvent polarity dependent changes in the Φ_{F} values for the four dyes respectively. For the dyes **4a** and **4b** the Φ_{F} values undergo very sharp decrease on increasing the solvent polarity. Such a large change in the Φ_{F} values with the solvent polarity strongly suggests that there is a large structural change for the present dyes following their photoexcitation in the excited state. The value of the fluorescence quantum yield is much lower in the compounds **5a** and **5b** (30% and 37%) compare to **4a** and **4b** (88% and 81%) even in non-polar solvents such as toluene. This concludes the functionalization of these groups also affects to the rigidity of the chromophore and hence, the structural properties have major influence in the deactivation of the radiative processes. The decrease in Φ_{F} values with increase in solvent polarity is more prominent in OBO complexes especially in dye **4b**. Dye **4b** has 81% quantum yield of

fluorescence in toluene where as in DMF, DMSO and acetonitrile it is below 3%. We thus propose that in the present cases the initially produced fluorescent states of BODIPY dyes along with local excitation (LE) undergo an intramolecular conversion to the highly polar intramolecular charge transfer (ICT) states which introduce additional nonradiative deexcitation for the excited dyes significantly their Φ_{F} values to drop sharply on increasing the solvent polarity.

Time-Resolved Fluorescence Spectroscopy

Time resolved fluorescence study was carried out in order to obtain the insight into the photo-induced processes involved in the excited states at the respective emission maxima of the dyes in different solvent. Values of average fluorescence lifetime (τ), the rate of radiative (k_{R}) and non-radiative decay (k_{NR}) of dyes are mentioned in Table 1. Fluorescence decays of the five BODIPY dyes in the solvents of different polarities are shown in Fig. 8a, b, c, d, e respectively. In most cases a single-exponential analysis was acceptable for the observed decays. However, a bi-exponential analysis was also necessary in some cases, for which the average lifetime (τ_{Φ}), as estimated by using Eq. 1 were considered as the lifetime of the fluorescent state of the dyes [24, 25].

$$\tau_{\Phi} = a_1\tau_1 + a_2\tau_2 \quad (1)$$

Table 1 Effect of solvent dielectric constant on the photophysical properties of the Dyes 4a, 4b, 5a and 5b

Solvents	ϵ_s^a	λ_{abs}^b [nm]	λ_{em}^c [nm]	ν^d [cm ⁻¹]	Φ_f^e	τ_{ϕ}^f [ns]	k_R^g (10 ⁹ s ⁻¹)	k_{NR}^h (10 ⁹ s ⁻¹)
4a								
Toluene	2.43	551	570	604	0.88	2.98	0.295	0.040
Ethyl acetate	6.02	545	565	649	0.79	3.02	0.263	0.069
THF	7.58	547	567	644	0.79	2.96	0.269	0.070
DCM	9.02	551	572	666	0.67	2.54	0.264	0.129
Ethanol	24.3	547	567	644	0.25	1.23	0.162	0.609
DMF	29	552	573	663	0.03	1.12	0.027	0.866
Methanol	33.6	546	567	678	0.07	0.45	0.156	2.066
ACN	37.5	544	568	776	0.06	0.53	0.112	1.773
DMSO	46.7	551	577	817	0.14	0.98	0.142	0.877
4b								
Toluene	2.43	565	585	605	0.81	2.67	0.303	0.071
Ethyl acetate	6.02	554	582	868	0.70	2.52	0.278	0.119
THF	7.58	562	586	728	0.73	2.47	0.296	0.109
DCM	9.02	567	595	829	0.26	1.33	0.195	0.556
Ethanol	24.3	562	586	728	0.05	–	–	–
DMF	29	567	596	858	0.03	–	–	–
Methanol	33.6	560	588	850	0.01	–	–	–
ACN	37.5	560	594	1022	0.01	–	–	–
DMSO	46.7	569	601	935	0.02	–	–	–
5a								
Toluene	2.43	542	584	1326	0.30	2.48	0.121	0.282
Ethyl acetate	6.02	535	578	1390	0.17	2.11	0.081	0.393
THF	7.58	537	579	1350	0.17	1.99	0.085	0.417
DCM	9.02	538	582	1405	0.20	1.84	0.109	0.434
Ethanol	24.3	535	578	1390	0.12	1.73	0.069	0.508
DMF	29	–	558	–	0.07	3.59	0.019	0.259
Methanol	33.6	534	567	1089	0.08	1.91	0.042	0.481
ACN	37.5	529	550	721	0.12	3.93	0.030	0.223
DMSO	46.7	537	555	603	0.09	3.65	0.025	0.249
5b								
Toluene	2.43	546	585	1221	0.37	2.49	0.149	0.253
Ethyl acetate	6.02	540	583	1365	0.20	1.75	0.114	0.457
THF	7.58	543	584	1292	0.21	1.77	0.118	0.446
DCM	9.02	544	584	1259	0.24	1.95	0.123	0.389
Ethanol	24.3	542	582	1268	0.14	1.31	0.106	0.656
DMF	29	541	589	1506	0.12	1.41	0.085	0.624
Methanol	33.6	540	584	1395	0.10	1.22	0.082	0.737
ACN	37.5	536	583	1504	0.11	1.56	0.070	0.570
DMSO	46.7	543	586	–	0.10	1.62	0.062	0.555
6								
Toluene	2.43	620	639	480	0.21	1.76	0.119	0.449
Ethyl acetate	6.02	612	633	542	0.15	1.76	0.085	0.483
THF	7.58	615	638	586	0.14	1.69	0.083	0.509
DCM	9.02	623	655	784	0.12	1.71	0.070	0.515
Ethanol	24.3	617	645	704	0.06	0.58	–	–
DMF	29	622	652	740	NA	0.02	–	–
Methanol	33.6	613	642	737	0.03	0.2	–	–
ACN	37.5	614	650	902	NA	0.003	–	–
DMSO	46.7	609	658	1223	NA	0.003	–	–

^asolvent dielectric constant, ^b Wavelength at absorption maximum, ^c Wavelength at emission maximum, ^d Stokes shift, ^e Fluorescence quantum yield, determined using PM567 in ethanol ($\phi_f=0.84$), Rh 101 in ethanol ($\phi_f=0.92$) and PM 597 in ethanol ($\phi_f=0.42$) as standard, ^f average fluorescence life time, ^g rate of radiative decay, ^h rate of nonradiative decay

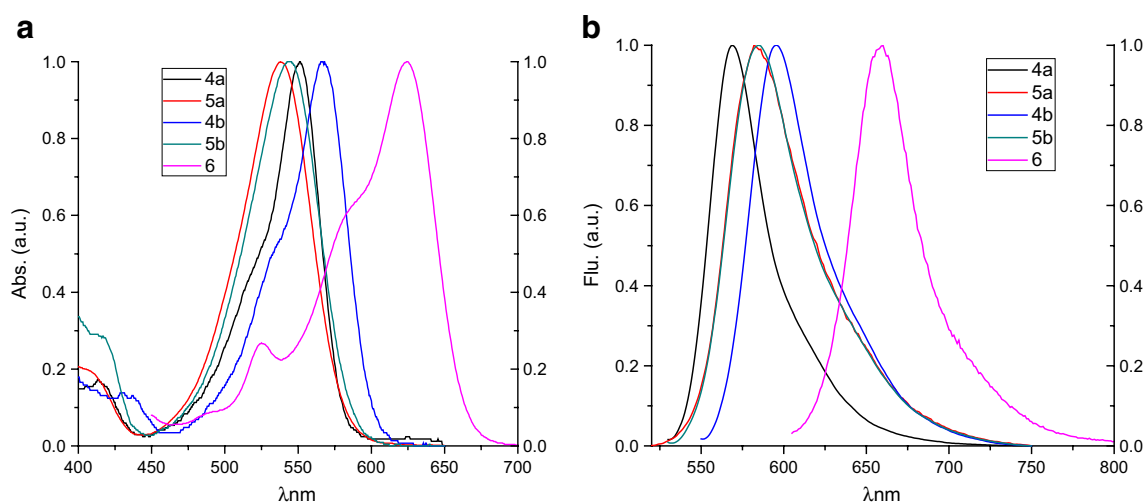


Fig. 1 Normalized absorption (a) and emission (b) spectra of BODIPY dyes **4a**, **4b**, **5a**, **5b**, and **6** in dichloromethane

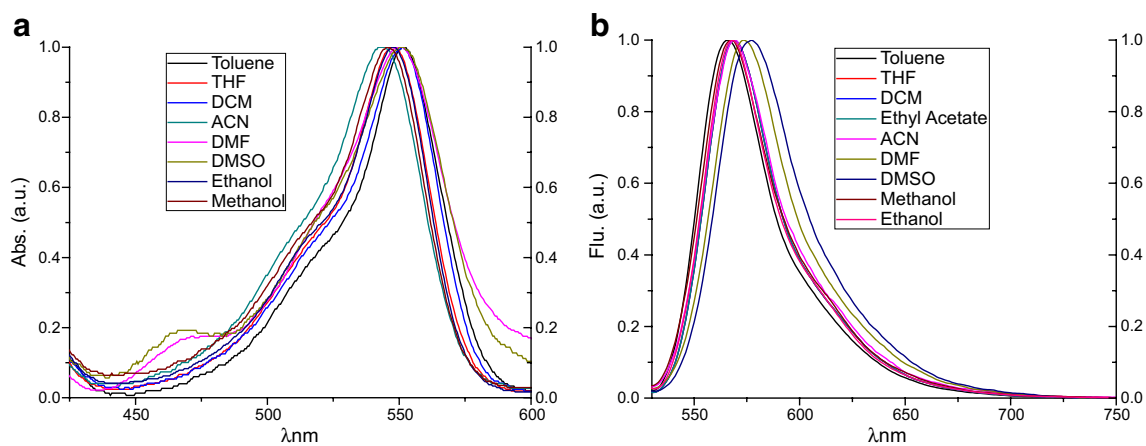


Fig. 2 Normalized absorption (a) and emission (b) spectra of BODIPY dyes **4a**, in various solvents

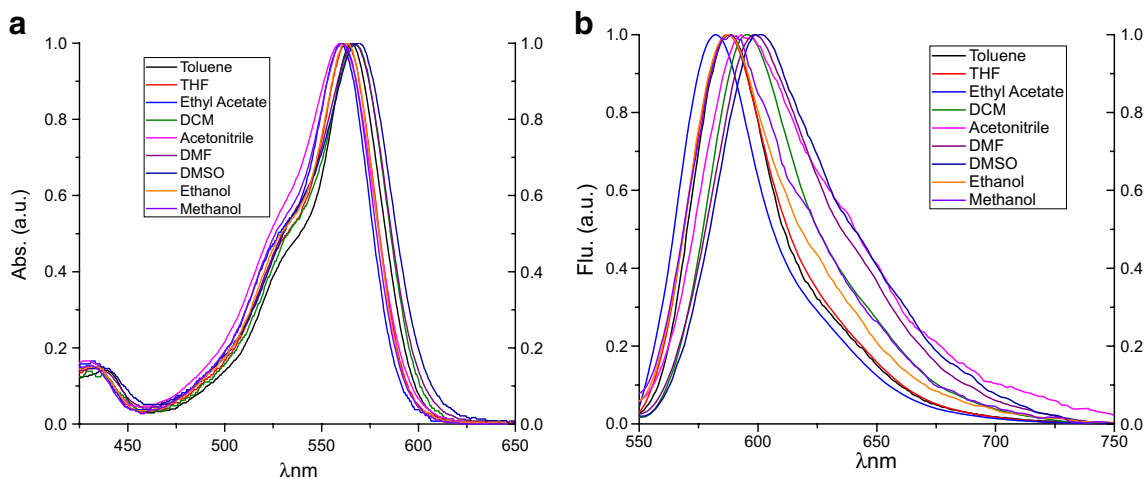


Fig. 3 Normalized absorption (a) and emission (b) spectra of BODIPY dyes **4b**, in various solvents

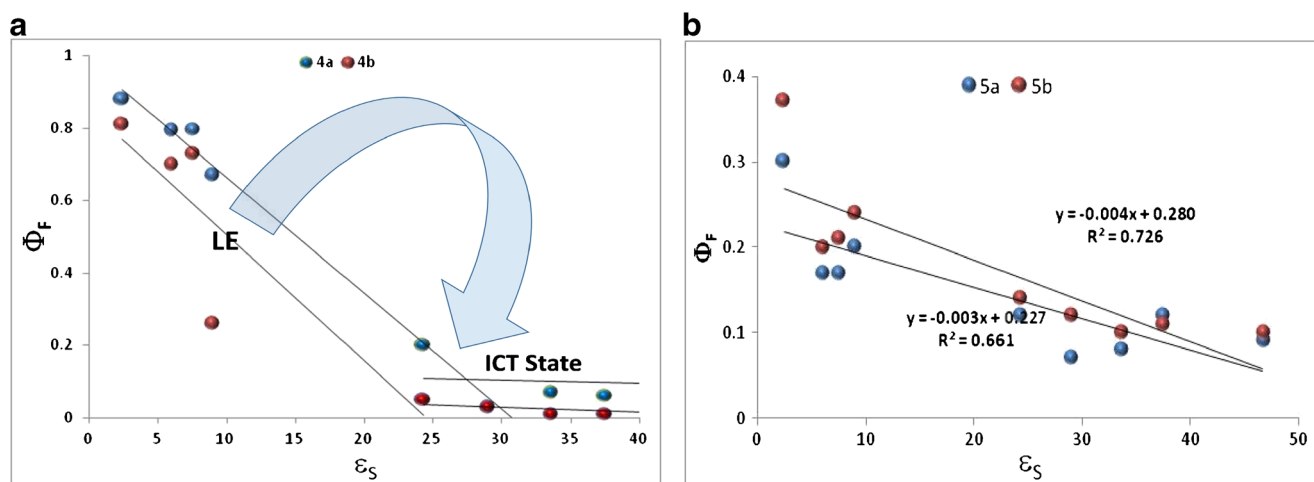


Fig. 4 change of fluorescence quantum yield (Φ_F) of the dyes **4a**, **4b** (a) and **5a**, **5b** (b) against solvent dielectric constant (ϵ_S)

Where, τ_1 and τ_2 are the two estimated fluorescence life times and α_1 and α_2 are their relative contributions in the observed decay. The average τ_Φ values of the four dyes in the solvents of different polarities are presented in Table 1. From Table 1 it has been seen that the fluorescence lifetime values decrease from non-polar to polar solvents. The low fluorescence intensity in polar solvents of BODIPY dye 4b restricts the measurement of fluorescence life time. The graphs of average fluorescence life time vs solvent dielectric constant have been plotted for dyes **4a**, **4b** and **5a**, **5b**, which are presented in Fig. 5. From Fig. 5 it has been seen that, the τ_Φ values of the four dyes also show very sharp decrease on increasing the solvent polarity and is very similar to the changes that observed with the Φ_F

values of the dyes. However for dyes **5a** uneven decrease in the τ_Φ values with Φ_F is observed.

For compounds **4a**, **4b**, **6** and to a smaller extent for **5a** and **5b** we observe that upon increasing the solvent polarity the fluorescence quantum yield decreases stronger than the fluorescence decay time. Upon increasing solvent polarity the formation of a non-fluorescent ICT state provides an extra decay channel through non-radiative pathway of the LE state that remains responsible for the emission. This explains the decrease in fluorescence decay time and a similar behavior has been observed for several other BODIPYs substituted by an electron acceptors or donor. The apparent decrease in the fluorescent rate constant can be explained in two ways

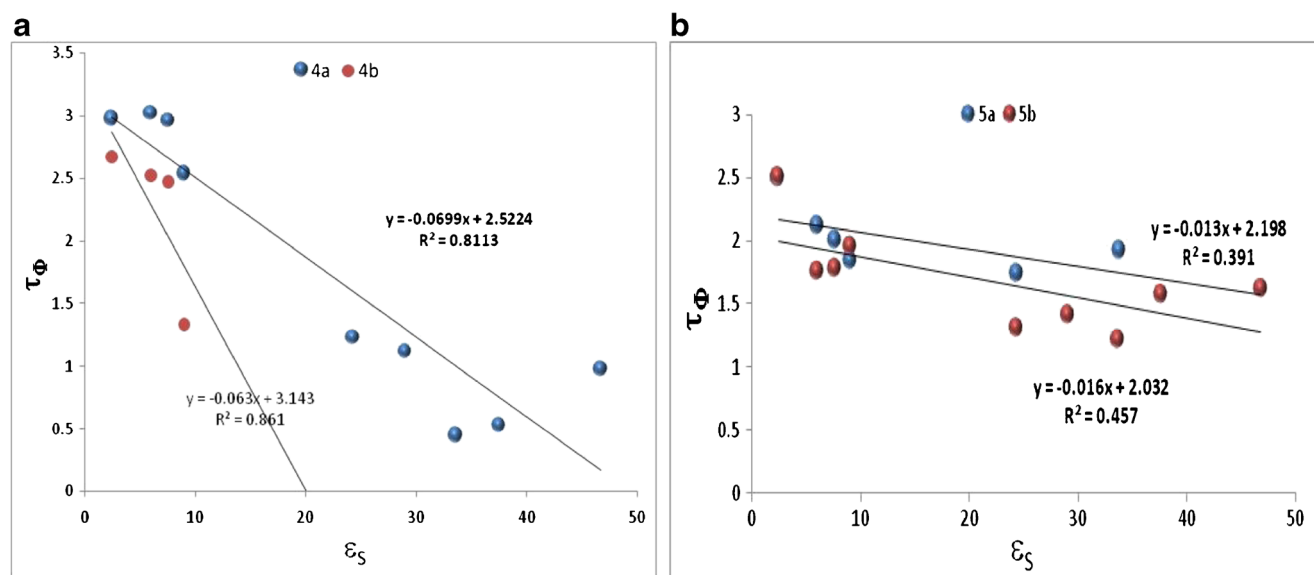


Fig. 5 change of fluorescence lifetime (τ_Φ) of the dyes **4a**, **4b** (a) and **5a**, **5b** (b) against solvent dielectric constant (ϵ_S)

- a) after excitation the Franck Condon excited state either forms a relaxed locally excited state responsible for the emission or an non fluorescent ICT state. Upon increasing solvent polarity the latter process becomes more efficient at the expense of the former.
- b) The equilibrium between the fluorescent locally excited state and the non-fluorescent ICT state is established on a time scale faster than the time resolution of the TCSPC set-up. The observed decay time is in this case an average between the decay time of the locally excited state and the ICT state.

These results are thus in support to our assumptions that there is a conversion of the fluorescent states to the highly polar ICT states that assist fast nonradiative de-excitation of the excited dyes. The formation of ICT states for the present dyes is fully supported by solvent polarity dependent changes in τ_Φ and Φ_{fl} values. Further to correlate these

propositions, estimated the radiative and non radiative rate constant in different solvents by using the following Eqs. 2 and 3.

$$k_R = \frac{\Phi_F}{\tau_\Phi} \quad (2)$$

$$k_{NR} = (1 - \Phi_F) / \tau_\Phi \quad (3)$$

From these two equations we estimated the k_R and k_{NR} values in solvents of varying polarities and presented in Table 1. The plots of k_R values vs solvent dielectric constant were plotted and presented in Fig. 6. Figure 6 shows sharp decrease in k_R values for the five dyes under investigation with increasing solvent polarity. These phenomena is quite common for the dyes having ICT character in their excited state [26]. Further, we plotted the graphs of k_{NR} values against solvent dielectric constant and presented in Fig. 7.

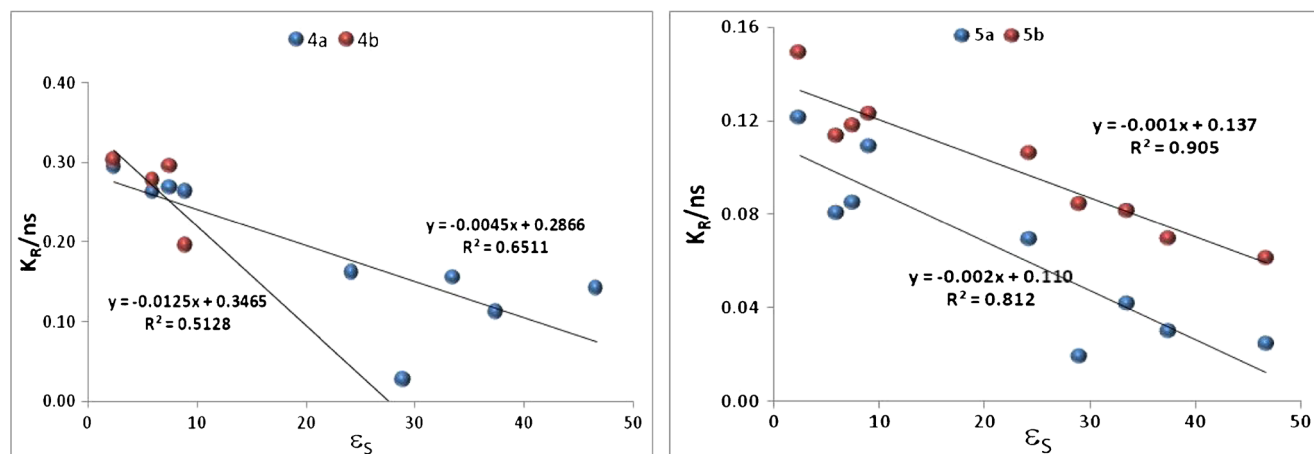


Fig. 6 Effect of solvent dielectric constant (ϵ_s) on the derived rate constant for radiative decay

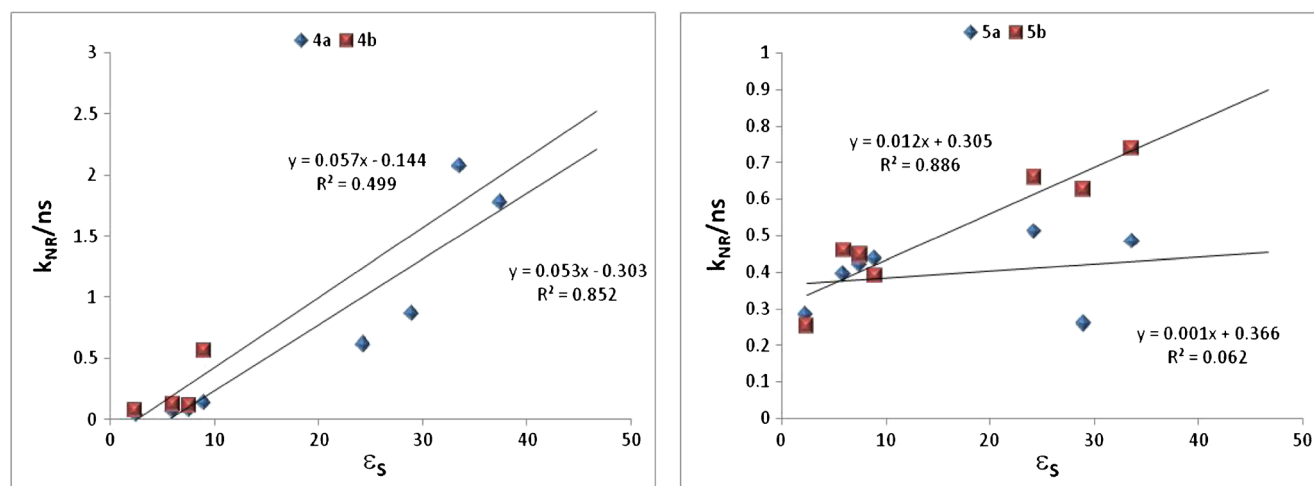


Fig. 7 Effect of solvent dielectric constant (ϵ_s) on the derived rate constant for nonradiative decay

With increase in solvent dielectric constant value the considerable increase in the k_{NR} values is observed for the **4a**, **4b**, **5b** and **6**. However, in case of BODIPY dye **4b** no such increase in k_{NR} values is observed. Also, from Table 1 it has been observed that for all the dyes the k_{NR} values are much higher than the k_R values in all solvents studied. Moreover, with increasing solvent polarity the

discrepancy between k_{NR} values and k_R values goes on increasing. The large k_{NR} values and their exponential increase with solvent polarity is a clear indication of the involvement of the highly polar ICT states as intermediates in the nonradiative deexcitation pathways of the fluorescent ICT states of the dyes under study [27] (Fig. 8).

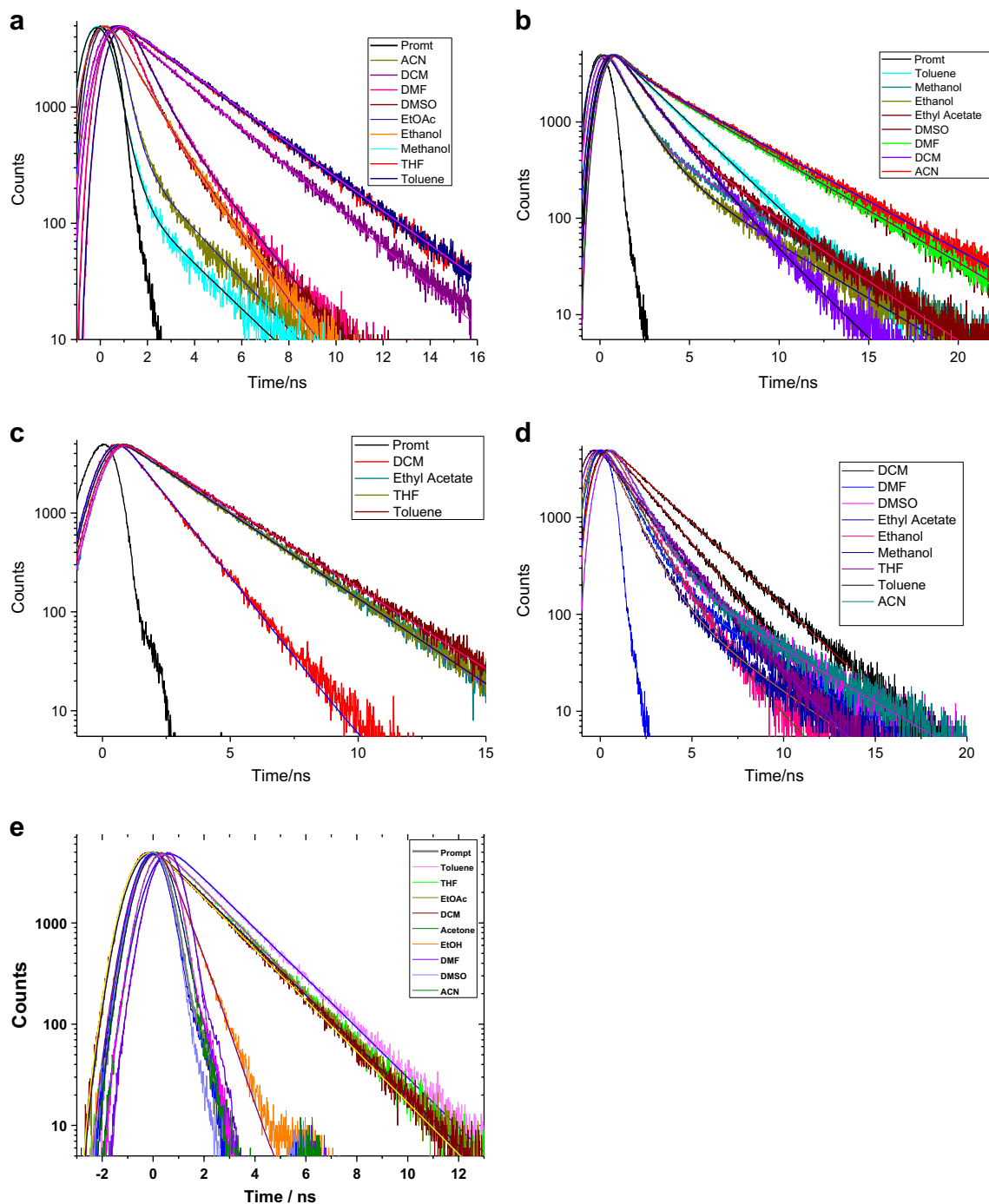


Fig. 8 a, b, c, d and e are the fluorescence lifetime decay curves of BODIPY dyes **4a**, **4b**, **5a**, **5b**, and **6**, respectively in solvents of varying polarities

Quantum Chemical Calculations

To get a better insight in the correlation of molecular structure and photophysical properties of the fluorophores, the geometries in ground (S_0) and excited state (S_1) of the BODIPY dyes were optimized with quantum chemical calculations using B3LYP 6-31G (d) and time-dependent DFT methods. The molecular orbital pictures of all five dye molecules in dichloromethane are shown in Fig. 9. For most of the reported BODIPY dyes the MO coefficients at meso-phenyl ring and at boron center are meager [28], the same we observed in the present finding. Figure 9 revealed that for all the five dye molecules the HOMO energy is spread over the whole molecule and is more centered on BODIPY unit (donor) in comparison with the acac or bzac and their respective BF_2 congeners (acceptor). Also, for the dyes **4b** and **5b** the phenyl ring of bzac unit is free from HOMO energy. However, in LUMO electron density is shifted from the donor BODIPY unit to the acceptor acac, bzac and their respective BF_2 congeners. For dye **4b** LUMO is more centered at OBO unit and phenyl ring of bzac which supports red emission of dye **4b**. Further, for BODIPY dimer **6** HOMO and LUMO are spread over the whole molecule with little difference resulting in red shifted absorption as well as emission maxima.

Experimental

4,4-Difluoro-1,3,5,7-tetramethyl-8-phenyl-4-bora-3a,4a-diaza-sindecene (1) Dye **1** was synthesized in 40% yield as reported earlier [20]. Red amorphous solid; mp: 178 °C; ^1H NMR (200 MHz, CDCl_3 , 25 °C, TMS): δ 1.36 (s, 6H), 2.54 (s, 6H), 5.97 (s, 2H), 7.25–7.28 (m, 2H), 7.44–7.48 (m, 3H); ^{13}C NMR: δ 14.2, 14.5, 121.2, 127.9, 128.5, 128.9, 129.1, 131.4, 134.9, 141.7, 143.1, 155.4; HRMS (ESI-TOF) m/z $[\text{M} + \text{H}]^+$ Calcd for $\text{C}_{19}\text{H}_{19}\text{BF}_2\text{N}_2$: 325.1687; Found: 325.1660.

2-Formyl-8-phenyl-1,3,5,7-tetramethyl-4-bora-3a,4a-diaza-s-indecene (2) Compound **2** was synthesized in 90% yield as reported earlier [29]. red solid; mp: >300 °C; ^1H NMR (500 MHz, CDCl_3 , 25 °C, TMS): δ 1.41 (s, 3H), 1.64 (s, 3H), 2.61 (s, 3H), 2.81 (s, 3H), 6.14 (s, 1H), 7.24–7.29 (m, 2H), 7.50–7.54 (m, 3H), 9.99 (s, 1H); ^{13}C NMR (125 MHz, CDCl_3 , 25 °C, TMS): δ 11.4, 12.9, 14.7, 15.0, 29.6, 124.0, 126.2, 127.6, 128.3, 129.4, 129.5, 129.9, 134.0, 142.8, 143.5, 147.3, 156.3, 161.6, 185.9; HRMS (ESI-TOF) m/z : $[\text{M} + \text{H}]^+$ Calcd. for $\text{C}_{20}\text{H}_{19}\text{BF}_2\text{N}_2\text{O}$: 353.1637; Found: 353.1604.

General synthesis procedure for 4a and 4b To a solution of **3a/3b** (1.40 mmol) in dry toluene (25 mL) was added **2** (100 mg, 0.28 mmol), tributyl borate (129 mg, 0.56 mmol)

and *n*-butylamine (8 mg, 0.10 mmol), the mixture was stirred at 70 °C under N_2 atmosphere. After completion of the reaction (16 h. cf. TLC), the mixture was brought to room temperature, filtered, washed with hexane and concentrated in vacuo. Column chromatography of the residue (silica gel, hexane/EtOAc, 80:10) furnished **4a/4b**.

Bodipy dye 4a (82 mg, 60%). orange solid; mp: 192 °C; ^1H NMR (500 MHz, CDCl_3 , 25 °C, TMS): δ 1.42 (s, 3H), 1.50 (s, 3H), 2.28 (s, 3H), 2.62 (s, 3H), 2.75 (s, 3H), 5.87 (s, 1H), 6.14 (s, 1H), 6.26 (d, $J = 15.0$ Hz, 1H), 7.26–7.30 (m, 2H), 7.54 (m, 3H), 8.05 (d, $J = 15.0$ Hz, 1H); ^{13}C NMR (125 MHz, CDCl_3 , 25 °C, TMS): δ 12.7, 14.4, 14.8, 15.1, 24.1, 101.0, 117.2, 121.8, 123.9, 127.8, 129.5, 129.6, 134.2, 140.2, 140.9, 142.7, 147.1, 155.3, 161.3, 180.7, 189.1; HRMS (ESI-TOF) m/z : $[\text{M} + \text{H}]^+$ Calcd. for $\text{C}_{25}\text{H}_{24}\text{B}_2\text{F}_4\text{N}_2\text{O}_2$: 483.2038; Found: 483.2037.

Bodipy dye 4b (78 mg, 65%). dark red solid MP: 225 °C; ^1H NMR (500 MHz, CDCl_3 , 25 °C, TMS): δ 1.42 (s, 3H), 1.52 (s, 3H), 2.61 (s, 3H), 2.78 (s, 3H), 6.13 (s, 1H), 6.42 (d, $J = 15$ Hz, 1H), 6.51 (s, 1H), 7.30 (m, 2H), 7.50 (m, 2H), 7.55 (m, 3H), 7.62 (m, 1H), 8.05 (m, 2H), 8.08 (d, $J = 15$ Hz). ^{13}C NMR: δ 12.6, 14.5, 14.8, 15.0, 97.55, 118.0, 123.8, 124.7, 127.8, 128.4, 128.9, 129.4, 129.5, 130.8, 132.2, 133.7, 134.2, 134.4, 139.7, 140.9, 142.6, 147.0, 155.3, 161.0, 180.3, 180.9, HRMS (ESI-TOF) m/z : $[\text{M} + \text{H}]^+$ Calcd for $\text{C}_{30}\text{H}_{26}\text{B}_2\text{F}_4\text{N}_2\text{O}_2$: 545.2195 Found: 545.2170.

General synthesis procedure for 5a and 5b The solution of **4a/4b** (0.20 mmol) in MeOH (5 mL) and DMSO (5 mL) was heated at 95 °C for 3 h. The mixture was brought to room temperature, H_2O (50 mL) added into it and extracted in CH_2Cl_2 (2 \times 10 mL). The organic layer was washed with H_2O (10 mL), concentrated in vacuo and the residue column chromatographed (silica gel, hexane/EtOAc, 80:20) to furnish **5a/5b**.

Bodipy dye 5a brown solid. 90% yield, MP: 205 °C; ^1H NMR: δ 1.38 (s, 3H), 1.48 (s, 3H), 2.58 (s, 3H), 2.75 (s, 3H), 6.06 (s, 1H), 6.23 (s, 1H), 6.27 (d, $J = 15.0$ Hz, 1H), 7.29 (m, 2H), 7.43–7.52 (m, 6H), 7.63 (d, $J = 15$ Hz, 1H), 7.91 (d, $J = 5$ Hz, 1H), ^{13}C NMR: δ 12.7, 14.2, 14.6, 14.8, 97.4, 122.7, 122.9, 125.6, 127.1, 127.9, 128.5, 129.2, 129.3, 131.6, 132.3, 132.7, 134.6, 136.1, 140.1, 142.2, 145.3, 154.6, 158.4, 180.7, 187.9. HRMS (ESI-TOF) m/z : $[\text{M} + \text{H}]^+$ Calcd for $\text{C}_{25}\text{H}_{25}\text{BF}_2\text{N}_2\text{O}_2$: 435.2055. Found: 435.2022.

Bodipy dye 5b 88% yield, MP: 259 °C; ^1H NMR: δ 1.38 (s, 3H), 1.48 (s, 3H), 2.58 (s, 3H), 2.75 (s, 3H), 6.06 (s, 1H), 6.23 (s, 1H), 6.27 (d, $J = 15$ Hz, 1H), 7.29 (m, 2H), 7.43–7.52 (m, 6H), 7.63 (d, $J = 15$ Hz, 1H), 7.91 (d, $J = 5$ Hz, 1H), ^{13}C NMR: δ 12.72, 14.27, 14.68, 14.85, 97.41, 122.71, 122.91, 125.69, 127.19, 127.93, 128.58, 129.29, 129.32, 131.66, 132.34, 132.71, 134.66, 136.13, 140.15, 142.28, 145.32, 154.63, 158.46, 180.75, 187.95.; HRMS (ESI-TOF)

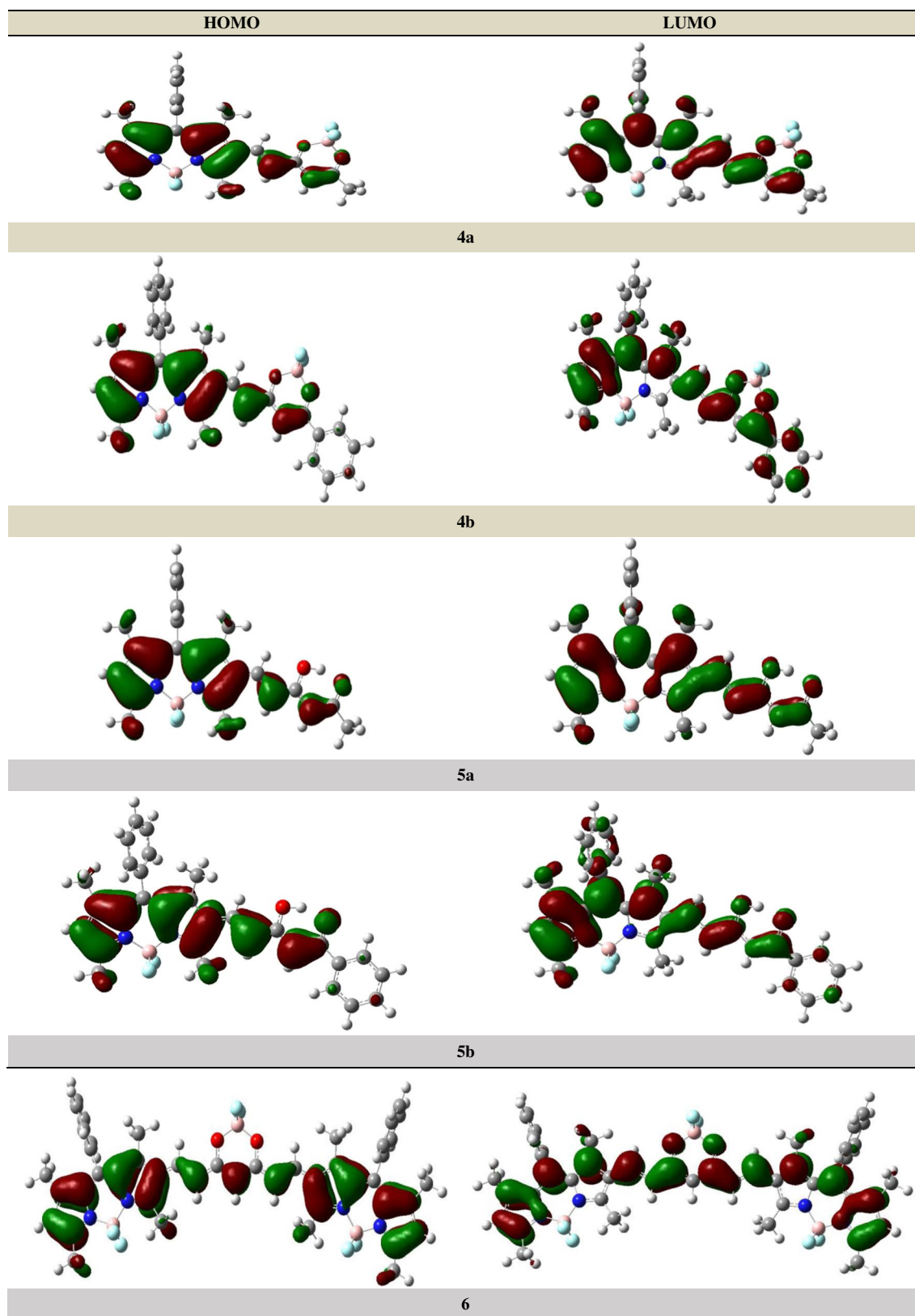


Fig. 9 DFT-optimized molecular structures of Dyes

m/z: [M + H] + Calcd for C₃₀H₂₇BF₂N₂O₂: 497.2212 Found: 497.2212.

Bodipy dye 6 Under nitrogen atmosphere, to a Schlenk tube was added **4a** (100 mg, 0.207 mmol), formyl BODIPY **3** (100 mg, 0.248 mmol), toluene (10 mL), tributyl borate (95 mg, 0.414 mmol) and n-butylamine (8 mg (10 μL), 0.1 mmol). The mixture was stirred at 70 °C for 16 h. After completion of the reaction monitored by TLC, the mixture was cooled to room temperature, filtered, washed with hexane followed by column chromatography of the residue (silica gel, hexane/ EtOAc) furnished copm.**6** as an dark red solid (78 mg, 65%). mp: 285 °C; ¹H NMR (500 MHz, DMSO, 100 °C): δ 1.45 (s, 6H), 1.54 (s, 6H), 2.56 (s, 6H), 2.72 (s, 6H), 6.39 (s, 2H), 6.58 (s, 1H), 6.59 (d, *J* = 15.0 Hz, 2H), 7.44 (m, 4H), 7.62 (m, 6H), 7.84 (d, *J* = 15.0 Hz, 1H); ¹³C NMR spectrum could not be obtained because of poor solubility HRMS (ESI-TOF) m/z: [M + H]⁺ Calcd. for C₄₅H₄₂B₃F₆N₄O₂: 817.3491; Found: 817.3472.

Conclusions

In summary, the influence of the electron accepting character of the acetyl acetone and benzoyl acetone BF₂ units and their respective curcuminoids congeners at β position of the BODIPY dyes is studied using UV-absorption, steady state and time-resolved fluorescence spectroscopy techniques, and supported by quantum chemical calculations. The effect of solvent polarity on the photophysical properties of the synthesized BODIPY dyes explain high rate of non-radiative decay in polar solvents due to the formation of ICT state.

Acknowledgements ABM sincerely thanks DAE-BRNS for the financial support.

References

- Chibani S, Charaf-Eddin A, Le Guennic B, Jacquemin D (2013) Boranil and related NBO dyes: insights from theory. *J Chem Theory Comput* 9:3127–3135. <https://doi.org/10.1021/ct400392r>
- Zhang Z, Achilefu S (2005) Design, synthesis and evaluation of near-infrared fluorescent pH indicators in a physiologically relevant range. *Chem Commun* 5887–5889. <https://doi.org/10.1039/B512315A>
- Boens N, Leen V, Dehaen W (2012) Fluorescent indicators based on BODIPY. *Chem Soc Rev* 41:1130–1172. <https://doi.org/10.1039/C1CS15132K>
- Prandi C, Ghigo G, Occhiato EG, Scarpi D, Begliomini S, Lace B, Alberto G, Artuso E, Blangetti M (2014) Tailoring fluorescent strigolactones for in vivo investigations: a computational and experimental study. *Org Biomol Chem* 12:2960–2968. <https://doi.org/10.1039/c3ob42592d>
- Kamkaew A, Lim SH, Lee HB, Kiew LV, Chung LY, Burgess K (2013) BODIPY dyes in photodynamic therapy. *Chem Soc Rev* 42:77–88. <https://doi.org/10.1039/C2CS35216H>
- Gong S, Liu Q, Wang X, Xia B, Liu Z, He W (2015) AIE-active organoboron complexes with highly efficient solid-state luminescence and their application as gas sensitive materials. *Dalton Trans* 44:14063–14070. <https://doi.org/10.1039/C5DT01525A>
- Mukherjee S, Thilagar P (2016) Stimuli and shape responsive “boron-containing” luminescent organic materials. *J Mater Chem C* 4:2647–2662. <https://doi.org/10.1039/C5TC02406D>
- Loudet A, Burgess K (2007) Dyes BODIPY and their derivatives: syntheses and spectroscopic properties. *Chem Rev* 107:4891–4932. <https://doi.org/10.1021/cr078381n>
- Zhu S, Bi J, Vegesna G, Zhang J, Luo F-T, Valenzano L, Liu H (2013) Functionalization of BODIPY dyes at 2,6-positions through formyl groups. *RSC Adv* 3:4793–4800. <https://doi.org/10.1039/C3RA22610G>
- Buyukcakir O, Bozdemir OA, Kolemen S, Erbas S, Akkaya EU (2009) Tetrastryl-bodipy dyes: convenient synthesis and characterization of elusive near IR fluorophores. *Org Lett* 11:4644–4647. <https://doi.org/10.1021/ol9019056>
- Mani V, Krishnakumar VG, Gupta S, Mori S, Gupta I (2017) Synthesis and characterization of styryl-BODIPY derivatives for monitoring in vitro Tau aggregation. *Sensors Actuators B Chem* 244:673–683. <https://doi.org/10.1016/j.snb.2016.12.104>
- Zhao N, Vicente MGH, Fronczek FR, Smith KM (2015) Synthesis of 3,8-dichloro-6-ethyl-1,2,5,7-tetramethyl-BODIPY from an asymmetric dipyrroketone and reactivity studies at the 3,5,8-positions. *Chemistry* 21 6181–6192. <https://doi.org/10.1002/chem.201406550>
- Lakshmi V, Ravikanth M (2014) Synthesis of hexasubstituted boron-dipyrromethenes having a different combination of substituents. *Eur J Org Chem* 2014 5757–5766. <https://doi.org/10.1002/ejoc.201402599>
- Rohand T, Baruah M, Qin W, Boens N, Dehaen W (2006) Functionalisation of fluorescent BODIPY dyes by nucleophilic substitution. *Chem Commun* 266–268. <https://doi.org/10.1039/B512756D>
- Dost Z, Atilgan S, Akkaya EU (2006) Distyryl-boradiazaindacenes: facile synthesis of novel near IR emitting fluorophores. *Tetrahedron* 62:8484–8488. <https://doi.org/10.1016/j.tet.2006.06.082>
- Kim E, Felouat A, Zaborova E, Ribierre J-C, Wu JW, Senatore S, Matthews C, Lenne P-F, Baffert C, Karapetyan A, Giorgi M, Jacquemin D, Ponce-Vargas M, Le Guennic B, Fages F, D'Aleo A (2016) Borondifluoride complexes of hemicurcuminoids as bio-inspired push-pull dyes for bioimaging. *Org Biomol Chem* 14:1311–1324. <https://doi.org/10.1039/C5OB02295A>
- Frisch MJ, Trucks GW, Schlegel HB, Scuseria GE, Robb MA, Cheeseman JR, Scalmani G, Barone V, Mennucci B, Petersson GA, Nakatsuji H, Caricato M, Li X, Hratchian HP, Izmaylov AF, Bloino J, Zheng G, Sonnenberg JL, Hada M, Ehara M, Toyota K, Fukuda R, Hasegawa J, Ishida M, Nakajima T, Honda Y, Kitao O, Nakai H, Vreven T, Montgomery JA, Peralta JE, Ogliaro F, Bearpark M, Heyd JJ, Brothers E, Kudin KN, Staroverov VN, Kobayashi R, Normand J, Raghavachari K, Rendell A, Burant JC, Iyengar SS, Tomasi J, Cossi M, Rega N, Millam JM, Klene M, Knox JE, Cross JB, Bakken V, Adamo C, Jaramillo J, Gomperts R, Stratmann RE, Yazyev O, Austin AJ, Cammi R, Pomelli C, Ochterski JW, Martin RL, Morokuma K, Zakrzewski VG, Voth GA, Salvador P, Dannenberg JJ, Dapprich S, Daniels AD, Farkas, Foresman JV, Ortiz J, Cioslowski, Fox DJ (2009) Gaussian 09, Revision C.01, Gaussian 09, Revis. B.01, Gaussian, Inc., Wallingford CT. citeulike-article-id:9096580
- Bauernschmitt R, Häser M, Treutler O, Ahlrichs R (1997) Calculation of excitation energies within time-dependent density functional theory using auxiliary basis set expansions. *Chem Phys Lett* 264:573–578. [https://doi.org/10.1016/S0009-2614\(96\)01343-7](https://doi.org/10.1016/S0009-2614(96)01343-7)

19. Becke AD (1993) Density functional thermochemistry. III. The role of exact exchange. *J Chem Phys* 98:5648–5652. <https://doi.org/10.1063/1.464913>
20. Yue Y, Guo Y, Xu J, Shao S (2011) A Bodipy-based derivative for selective fluorescence sensing of homocysteine and cysteine. *New J Chem* 35:61–64. <https://doi.org/10.1039/C0NJ00720J>
21. Jiao L, Yu C, Li J, Wang Z, Wu M, Hao E (2009) β -formyl-BODIPYs from the Vilsmeier-Haack reaction. *J Org Chem* 74:7525–7528. <https://doi.org/10.1021/jo901407h>
22. Liu K, Chen J, Chojnacki J, Zhang S (2013) $\text{BF}_3 \cdot \text{OEt}_2$ -promoted concise synthesis of difluoroboron-derivatized curcumins from aldehydes and 2,4-pentanedione. *Tetrahedron Lett* 54:2070–2073. <https://doi.org/10.1016/j.tetlet.2013.02.015>
23. More AB, Mula S, Thakare S, Chakraborty S, Ray AK, Sekar N, Chattopadhyay S (2017) An acac-BODIPY dye as a reversible “ON-OFF-ON” fluorescent sensor for Cu^{2+} and S^{2-} ions based on displacement approach. *J Lumin* 190:476–484. <https://doi.org/10.1016/j.jlumin.2017.06.005>
24. Satpati AK, Kumbhakar M, Nath S, Pal H (2008) Photoinduced electron transfer between quinones and amines in micellar media: tuning the Marcus inversion region. *J Photochem Photobiol A Chem* 200:270–276. <https://doi.org/10.1016/j.jphotochem.2008.08.001>
25. Shaikh M, Pal H (2014) Photophysics of donor-acceptor kind of styryl dyes: involvement of twisted intramolecular charge transfer (TICT) state and the effect of solvent polarity
26. Saroja G, Soujanya T, Ramachandram B, Samanta A (1998) 4-Aminophthalimide derivatives as environment-sensitive probes. *J Fluoresc* 8:405–410. <https://doi.org/10.1023/A:1020536918438>
27. Pham THN, Clarke RJ (2008) Solvent dependence of the photochemistry of the styrylpyridinium dye RH421. *J Phys Chem B* 112:6513–6520. <https://doi.org/10.1021/jp711694u>
28. Popere BC, Della Pelle AM, Thayumanavan S (2011) BODIPY-based donor-acceptor π -conjugated alternating copolymers. *Macromolecules* 44:4767–4776. <https://doi.org/10.1021/ma200839q>
29. More AB, Mula S, Thakare S, Sekar N, Ray AK, Chattopadhyay S (2014) Masking and Demasking Strategies for the BF_2 -BODIPYs as a Tool for BODIPY Fluorophores. *J Org Chem* 79:10981–10987. <https://doi.org/10.1021/jo502028g>